Int J Adv Manuf Technol (2006) 27: 518–524
DOI 10.1007/s00170-004-2204-6

ORIGINAL ARTICLE

Jeong Kim · Sang-Woo Kim · Hoon-Jae Park · Beom-Soo Kang

A prediction of bursting failure in tube hydroforming process based on plastic instability

Received: 8 March 2004 / Accepted: 6 April 2004 / Published online: 19 January 2005

Abstract Based on plastic instability, an analytical prediction of bursting failure on tube hydroforming processes under combined internal pressure and independent axial feeding is carried out. Bursting is an irrecoverable phenomenon due to local instability under excessive tensile stresses. In order to predict the bursting failure, three different classical necking criteria – diffuse necking criteria for a sheet, and a tube, and a local necking criterion for a sheet – are introduced. The incremental theory of plasticity for an anisotropic material is adopted and the hydroforming limit, as well as a diagram of bursting failure with respect to axial feeding and hydraulic pressure are presented. In addition, the influences of material properties such as anisotropy parameter, strain hardening exponent and strength coefficient on plastic instability and bursting pressure are investigated. As a result of the above approach, the hydroforming limit with respect to bursting failure is verified with experimental results.

Keywords Diffuse necking · Hydroforming · Local necking · Plastic anisotropy · Plastic instability · Tube bulge

1 Introduction

Recently, hydroforming technology has been widely used in the mass production of lightweight components for the automotive and aircraft industries [1]. Tube hydroforming offers several advantages as compared to conventional manufacturing via a stamping process, including weight reduction, improved structural strength, lower tooling cost, and so on. In hydroforming operations, tubular components are hydrobulged or hydroformed from tubular blanks with internal pressure and simultaneous axial loading. The internal pressure shapes the tube in the form of the die and the axial feeding applied to the ends of the blank prevent premature necking due to wall-thinning. If these axial forces are too large, buckling of the tube may occur. Successful tubular hydroforming depends on a reasonable combination of the internal pressure and the axial compression force at the tube ends. By contrast with buckling, which can be eliminated during the final calibration stage, bursting, which is a due to local instability under the influence of large tensile forces, is an irrecoverable failure mode. Thus, the prediction of the start of necking and the effects of the process parameters on this failure condition are an important issue in hydroforming processes.

Even though there are many different criteria that determine the bursting failure in hydroforming processes, their validation with experiments and practical implementation has not yet been solidly proved. Since the bursting is a consequence of necking, which is a condition of local instability under excessive tensile forces, the studies on prediction of this failure in hydroforming processes based on plastic instability are proceeding. The well-known diffuse necking criterion for a closed-end tube can be deduced from Hill's uniqueness principle, as in Yamada and Aoki [2]. This criterion was applied to the hydroforming process by Xing and Makinouchi [3]. Tirosh et al. [4] and Xia [5] presented an analytical simplified prediction of bursting as well as for buckling instability simultaneously. Nefussi and Combescure [6] discussed Swift's two criteria for sheet-forming and for tube hydroforming where necking and buckling are considered simultaneously. For specific industrial purposes, these analytical approaches provide simple but useful guidelines for product designers and process engineers to avoid failure during the hydroforming operation. However, even though a few previous works take into account plastic anisotropy of the tube material, the influences on the bursting failure are not investigated. Also, the

J. Kim · S.-W. Kim
Department of Aerospace Engineering,
Pusan National University,
Busan 609-735, Korea

H.-J. Park
Manufacturing Process Research Center,
Korea Institute of Industrial Technology,
Chonan 330-825, Korea

B.-S. Kang (✉)
ERC/NSDM,
Pusan National University,
Busan 609-735, Korea
E-mail: bskang@pusan.ac.kr
Tel.: +82-51-5102310
Fax: +82-51-5133760

hydroforming limit obtained from their approaches has not been verified with experimental results at all.

In Sect. 3.2, three different criteria – two diffuse necking criteria and a local necking criterion – are introduced in order to investigate their potential for application in the prediction of limit strain and bursting pressure. Next, diagrams of the hydroforming limit and bursting pressure with respect to axial feeding and hydraulic pressure are presented and are confirmed by a series of tube bulging tests.

In Sect. 5, the influences of the material properties such as anisotropy parameter, R, strain hardening exponent, n, and strength coefficient, K, on plastic instability and bursting pressure are investigated.

Consequently, it is shown that this approach will provide a feasible method to satisfy the increasing practical demands for evaluating formability in hydroforming processes.

2 Experiments

In order to evaluate the forming limit of the hydroforming process and verify the analytical approach proposed in this paper, a series of tube bulging tests are executed. The tube material is assumed to obey the stress-strain relationship $\bar{\sigma} = 1400\,\bar{\varepsilon}^{0.17}$ (MPa) and have a normal anisotropy with anisotropy value $R = 2.14$. This test uses internal hydraulic pressure to bulge a tube that is supported between a lower and an upper die. The lower part of the tube is fixed, while the other is free to move in the downward direction. This condition can provide axial feeding during the test. The dimensions and configurations of the die and final bulged part are shown in Fig. 1. In order to observe bursting failure, high internal pressures under a relatively small axial feeding displacement as shown in Fig. 2 are applied. The internal pressures and the axial feeding displacements in Fig. 2 are

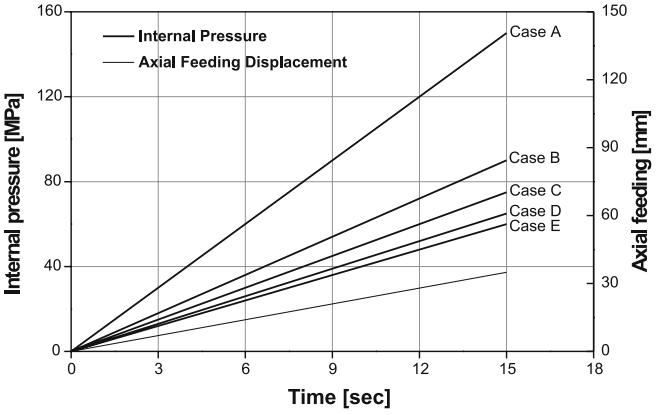

Fig. 2. Input loading paths with five different cases

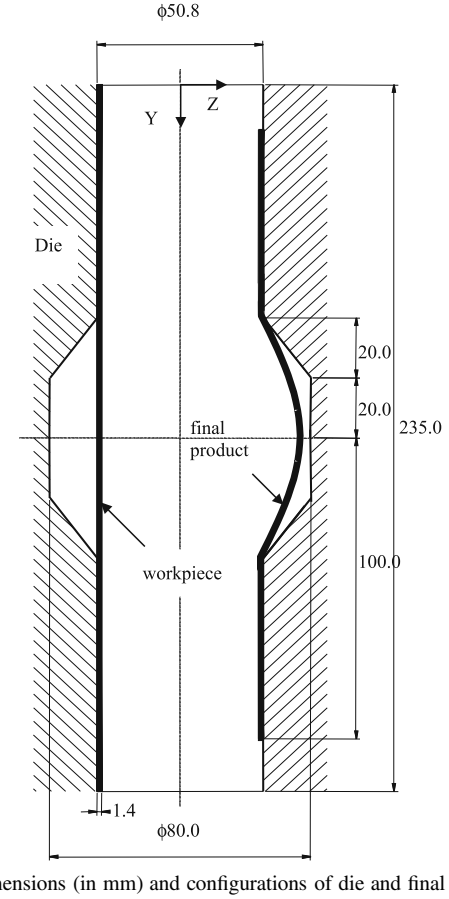

Fig. 1. Dimensions (in mm) and configurations of die and final bulged part

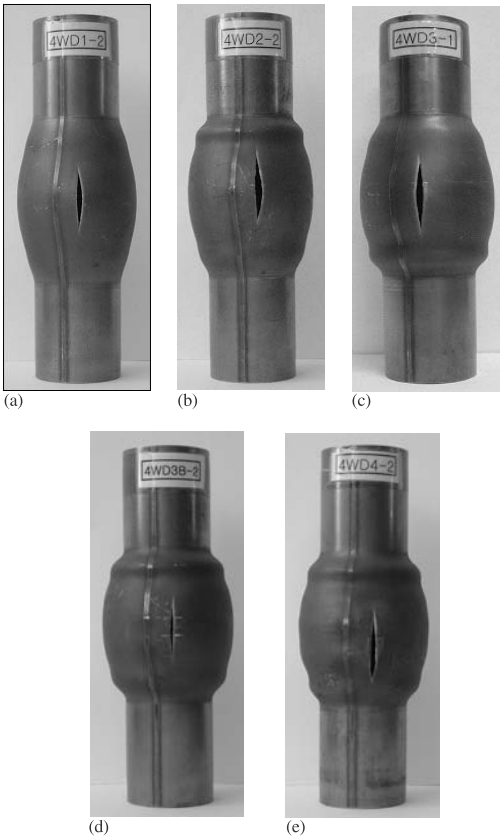

Fig. 3a–e. Experimental bursting failure obtained from bulge tests under different loading paths. **a** Case A. **b** Case B. **c** Case C. **d** Case D. **e** Case E

Table 1. Measured bursting pressure values and axial feeding displacements

Case	Bursting pressure value [MPa]	Axial feeding displacement [mm]
A	58.0	13
B	56.0	19
C	53.0	21
D	52.0	28
E	50.0	27

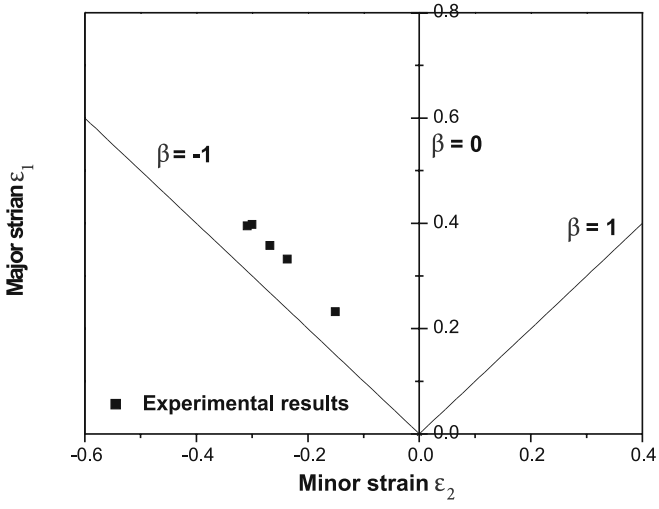

Fig. 4. Hydroforming limit diagram obtained experimentally

the input loading paths, which are controlled by a PC-based controller in the experimental set-up for a specified process sequence for a series of bulging tests. In addition, the process parameters can be stored and visualized on the PC. As a result of excessive pressurizing during the bulging process, bursting occurs at the middle of the tube wall as illustrated in Fig. 3. For all cases, bursting appears at a welding seam line of the tube. Since the work hardening of the heat affected zone (HAZ) is lower than that of the base metal, it is shown that initial fracture takes place at the HAZ near the welding line [7]. Table 1 lists the bursting pressure values and the corresponding axial displacements for each case. Figure 4 shows the limit strains, plotted as black square dots, experimentally obtained form bulge tests.

3 Theory

3.1 Incremental theory of plasticity for an anisotropic material

Consider a thin-walled, closed-end tube with original thickness t_o and radius r_o under internal hydraulic pressure p and axial load P, which are applied independently. The tube is assumed to be thin enough for the plane stress hypothesis to be valid and to maintain the orthogonal anisotropic character along the axial and the hoop directions. From the constitutive equation, the ratios of the plastic strain increment are defined by

$$d\varepsilon_{ij} = \frac{\partial f(\bar{\sigma}, Y)}{\partial \sigma_{ij}} d\lambda \tag{1}$$

where λ is the plastic multiplier and f is the plastic potential identified as the scalar function that defines the elastic limit surface.

From Hill's quadratic yield criterion for anisotropic materials [8]

$$\begin{aligned} 2f(\sigma_{ij}) =& F(\sigma_y - \sigma_z)^2 + G(\sigma_z - \sigma_x)^2 + H(\sigma_x - \sigma_y)^2 \\ &+ 2L\tau_{yz}^2 + 2M\tau_{zx}^2 + 2N\tau_{xy}^2 = 1 \end{aligned} \tag{2}$$

where $\bar{\sigma}$ is the effective stress, Y is the yield stress in simple tension and F, G, H, L, M, and N are the anisotropy parameters.

For normal anisotropic materials, the following relationship between the anisotropy parameters, $N = F + 2H = G + 2H$, $L = M$, is satisfied. More frequently, the anisotropy of a material in Eq. 2 is represented by the quantities $R = \frac{H}{G} = \frac{H}{F}$. Then, under the plane stress condition, the effective stress for planar isotropic materials can be written as follows

$$\bar{\sigma} = \sqrt{\sigma_1^2 + \sigma_2^2 - \frac{2R}{R+1}\sigma_1\sigma_2} \tag{3}$$

where σ_1 and σ_2 are the principal hoop and axial stress, and R is an anisotropy parameter.

The plastic strain increments are given by considering the normality condition, incompressibility condition, and the equivalent work definition of the effective strain increment as follows

$$\begin{aligned} d\bar{\varepsilon} &= \frac{1+R}{\sqrt{1+2R}}\sqrt{d\varepsilon_1^2 + d\varepsilon_2^2 + \frac{2R}{R+1}d\varepsilon_1 d\varepsilon_2} \\ d\varepsilon_1 &= \frac{d\bar{\varepsilon}}{\bar{\sigma}}\left[\sigma_1 - \frac{R}{1+R}\sigma_2\right] \\ d\varepsilon_2 &= \frac{d\bar{\varepsilon}}{\bar{\sigma}}\left[\sigma_2 - \frac{R}{1+R}\sigma_1\right] \\ d\varepsilon_3 &= -(d\varepsilon_1 + d\varepsilon_2) \end{aligned} \tag{4}$$

where $d\varepsilon_1$, $d\varepsilon_2$, and $d\varepsilon_3$ are the plastic strain incremental components along the principal hoop, axial, and thickness directions, respectively.

3.2 Plastic instability criteria

The tube is long enough for the stresses to be assumed uniformly distributed. From the equilibrium equations

$$\sigma_1 = \frac{pr}{t} \text{ and } \sigma_2 = \frac{P + \pi r^2 p}{2\pi r t} \tag{5}$$

where P is negative when the axial force is compressive, and r and t are the current values of the tube's radius and wall thickness ($t \ll r$). Assuming that principal stresses maintain constant ratios and directions, the ratio of strain increments also will not change, i.e., $\alpha = \sigma_2/\sigma_1$, $\beta = d\varepsilon_2/d\varepsilon_1$. As a plastic instability condition, three different necking criteria are proposed.

3.2.1 Diffuse necking criterion for a sheet

The first assumption is that the condition for plastic instability is satisfied when the load reaches a maximum value along both principal directions: $dF_1 = 0$ and $dF_2 = 0$, with $F_1 = P + \pi r^2 p$ and $F_2 = prl$. This condition leads to the following simultaneous constraints : $d\sigma_1 = \sigma_1 d\varepsilon_1$ and $d\sigma_2 = \sigma_2 d\varepsilon_2$ [9].

From Eq. 4 and the plastic instability constraints, the variation of the principal stress components in terms of the principal hoop stress can be written as

$$d\sigma_1 = \frac{d\bar{\varepsilon}}{\bar{\sigma}}\left[\sigma_1 - \frac{R}{1+R}\sigma_2\right]\sigma_1 = \frac{d\bar{\varepsilon}}{\bar{\sigma}}\left[1 - \frac{\alpha\rho}{2}\right]\sigma_1^2$$
$$d\sigma_2 = \frac{d\bar{\varepsilon}}{\bar{\sigma}}\left[\sigma_2 - \frac{R}{1+R}\sigma_1\right]\sigma_2 = \frac{d\bar{\varepsilon}}{\bar{\sigma}}\alpha\left[\alpha - \frac{\rho}{2}\right]\sigma_1^2 \tag{6}$$

where $\rho = \frac{2R}{1+R}$.

Based on Eqs. 3 and 6, the variation of the effective stress is deduced to be

$$d\bar{\sigma} = \bar{\sigma} d\bar{\varepsilon}\left[\frac{\alpha(2\alpha-\rho)^2 + (2-\alpha\rho)^2}{4(1-\alpha\rho+\alpha^2)^{3/2}}\right] \tag{7}$$

Thus, the following instability criterion in terms of the sub-tangent Z for anisotropic materials is obtained

$$\frac{1}{Z_D} = \frac{1}{\bar{\sigma}}\frac{d\bar{\sigma}}{d\bar{\varepsilon}} \le \frac{\alpha(2\alpha-\rho)^2 + (2-\alpha\rho)^2}{4(1-\alpha\rho+\alpha^2)^{3/2}} \tag{8}$$

3.2.2 Diffuse necking criterion for a tube

As the second instability condition, it is assumed that plastic instability occurs when $dp = 0$ and $dP = 0$ simultaneously. This leads to the following simultaneous constraints: $d\sigma_1 = \sigma_1(2d\varepsilon_1 + d\varepsilon_2)$ and $d\sigma_2 = \sigma_1 d\varepsilon_1 + \sigma_2 d\varepsilon_2$ [9].

From Eq. 4 and the above constraints, the variation of the principal stress components in terms of the principal hoop stress can be written as

$$d\sigma_1 = \frac{d\bar{\varepsilon}}{\bar{\sigma}}\left[\left(2 - \frac{\rho}{2}\right) + \alpha(1-\rho)\right]\sigma_1^2$$
$$d\sigma_2 = \frac{d\bar{\varepsilon}}{\bar{\sigma}}\left[1 - \alpha\rho + \alpha^2\right]\sigma_1^2 \tag{9}$$

From Eqs. 3 and 9, the variation of the effective stress can be derived as

$$d\bar{\sigma} = \bar{\sigma} d\bar{\varepsilon}\left[\frac{\alpha(2\alpha-\rho)^2 + 2(2-\alpha\rho)(2-\alpha\rho+2\alpha-\rho)}{4(1-\alpha\rho+\alpha^2)^{3/2}}\right] \tag{10}$$

Thus, the plastic instability condition in terms of the sub-tangent Z for tube hydroforming is found to be

$$\frac{1}{Z_H} = \frac{1}{\bar{\sigma}}\frac{d\bar{\sigma}}{d\bar{\varepsilon}} \le \frac{\alpha(2\alpha-\rho)^2 + 2(2-\alpha\rho)(2-\alpha\rho+2\alpha-\rho)}{4(1-\alpha\rho+\alpha^2)^{3/2}} \tag{11}$$

3.2.3 Local necking criterion for a sheet

Hill's local necking criterion is introduced as the third plastic instability condition and the onset of plastic instability is assumed to occur when the following constraint is satisfied: $d\sigma_1 = \sigma_1(d\varepsilon_1 + d\varepsilon_2)$. Assuming that the stress ratio remains fixed, the deformation of the neck, $d\sigma_2 = \sigma_2(d\varepsilon_1 + d\varepsilon_2)$ is also satisfied [7].

From Eq. 4 and the instability constraints mentioned previously, the variation of the principal stress can be written as

$$d\sigma_1 = \frac{d\bar{\varepsilon}}{\bar{\sigma}}\left[(\alpha+1)\left(1 - \frac{\rho}{2}\right)\right]\sigma_1^2$$
$$d\sigma_2 = \frac{d\bar{\varepsilon}}{\bar{\sigma}}\left[\alpha(\alpha+1)\left(1 - \frac{\rho}{2}\right)\right]\sigma_1^2 \tag{12}$$

Based on Eqs. 3 and 12, the variation of the effective stress is deduced to be

$$d\bar{\sigma} = \bar{\sigma} d\bar{\varepsilon}\left[\frac{(1+\alpha)(2-\rho)}{2(1-\alpha\rho+\alpha^2)^{1/2}}\right] \tag{13}$$

Thus, the plastic instability criterion based on the local necking is found to be

$$\frac{1}{Z_L} = \frac{1}{\bar{\sigma}}\frac{d\bar{\sigma}}{d\bar{\varepsilon}} \le \frac{(1+\alpha)(2-\rho)}{2(1-\alpha\rho+\alpha^2)^{1/2}} \tag{14}$$

3.3 Analytical model on onset of bursting condition of tube hydroforming

To obtain forming limit curves in terms of strains for the above three cases, it is necessary to introduce the critical principal strains ε_1^c, ε_2^c along the hoop and the axial direction, respectively. With the work-hardening law, $\bar{\sigma} = K\bar{\varepsilon}^n$, Eqs. 8, 11 and 14 can be written as

$$\frac{1}{Z_i} = \frac{1}{\bar{\sigma}}\frac{d\bar{\sigma}}{d\bar{\varepsilon}} = \frac{n}{\bar{\varepsilon}} = \frac{\boldsymbol{\Psi}_i}{\boldsymbol{\Omega}_i} \ (i = D, H, L) \tag{15}$$

Assuming proportional loading, the equivalent strain can be described by

$$\bar{\varepsilon} = \frac{1+R}{\sqrt{1+2R}}\sqrt{\varepsilon_1^2 + \varepsilon_2^2 + \frac{2R}{R+1}\varepsilon_1\varepsilon_2} = \boldsymbol{\Theta}\varepsilon_1 \tag{16}$$

where

$$\boldsymbol{\Theta} = \frac{1+R}{\sqrt{1+2R}}\sqrt{1+\beta\rho+\beta^2}$$

According to Eqs. 15 and 16, the limit strains based on the plastic instability yield is found to be

$$\varepsilon_1^c = \frac{\boldsymbol{\Omega}_i n}{\boldsymbol{\Theta}\boldsymbol{\Psi}_i}$$
$$\varepsilon_2^c = \beta\varepsilon_1^c \tag{17}$$

Also, the bursting pressure p^c is determined from Eq. 5 to be

$$p^c = \frac{t^c}{r^c}\sigma_1^c \tag{18}$$

where t^c and r^c are current tube thickness and radius at the onset of necking, respectively, and are derived to be

$$t^c = t_o e^{-(\varepsilon_1^c+\varepsilon_2^c)}$$
$$r^c = r_o e^{\varepsilon_1^c} \tag{19}$$

From Eq. 4, σ_1^c, σ_2^c, the hoop and axial stress when the bursting failure occurs, can be obtained from the following

$$\sigma_1^c = \frac{(1+R)^2}{1+2R}\frac{\bar{\sigma}}{\bar{\varepsilon}}\left[\varepsilon_1^c + \frac{R}{1+R}\varepsilon_2^c\right]$$
$$\sigma_2^c = \frac{(1+R)^2}{1+2R}\frac{\bar{\sigma}}{\bar{\varepsilon}}\left[\varepsilon_2^c + \frac{R}{1+R}\varepsilon_1^c\right] \tag{20}$$

From Eqs. 18 and 20, the bursting pressure can be written as follows

$$p^c = \frac{(1+R)^2}{1+2R}\frac{\bar{\sigma}}{\bar{\varepsilon}}\frac{t}{r}\left[\varepsilon_1^c + \frac{R}{1+R}\varepsilon_2^c\right] \tag{21}$$

4 Verification with experimental results

The results for three different plastic instability conditions assumed in this paper are represented in Figs. 5 and 6. From Fig. 5, we conclude that (i) the forming limit of tube hydroforming based on diffuse necking criterion for tube is the closest to the experimental forming limit compared to the others; and (ii) the forming limit based on the local necking criterion for a sheet overestimates the major strain limit compared with the experimental results while the forming limit based on the diffuse necking criterion for a sheet underestimates the limit strain.

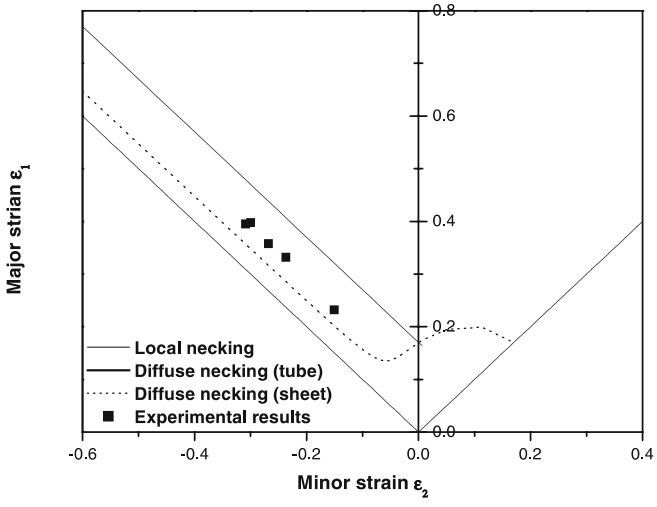

Fig. 5. Comparison of predicted and measured forming limit

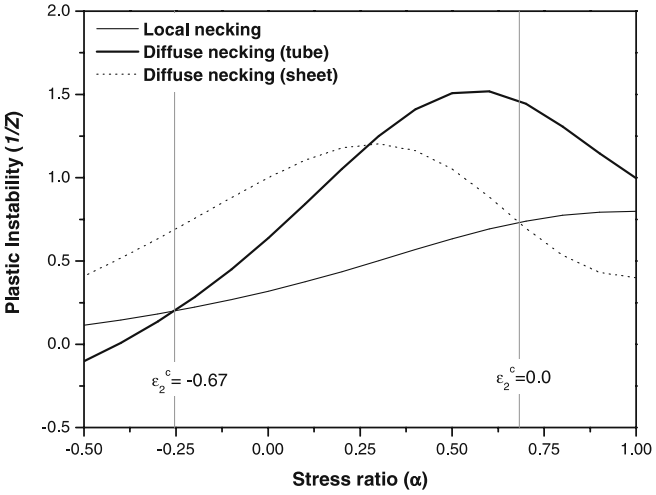

Fig. 6. Plastic instability $1/Z$ for various necking criteria

Result (i) can be explained from the assumptions employed in each plastic instability criterion. Local necking criterion assumes that necking occurs in the direction perpendicular to the circumference, and on the necking band, the strain in that direction is expected to be zero. However, the experiments carried out in this study adopt not only internal pressure but also axial feeding, which results in a negative minor strain in the direction perpendicular to the circumference. In the case of the diffuse necking criterion for a sheet, it is assumed that necking occurs when the load reaches the maximum along both principal directions. However, this condition is not an easy situation to enforce in the tube hydroforming process [6]. By reason of the assumptions involved in each necking criterion, the diffuse necking criterion for a tube, which postulates that necking occurs when the internal pressure and axial feeding force reach extreme values, shows good agreement with the experimental results.

The limit strains for all three necking criteria proposed in this paper are obtained analytically from the Eq. 17. Only the term $\frac{\Omega_i}{\Psi_i}$ in Eq. 17 is dependent on the plastic instability criteria and also it can be expressed in terms of $1/Z_i$, as in Eq. 15. Thus, result (ii) can be explained from plastic instability, expressed as $1/Z$, for the three necking criteria represented in Fig. 6. As shown in Fig. 6, the plastic instability curve based on the local necking criterion is lower than the others within the range of $\varepsilon_2^c = -0.67$ to $\varepsilon_2^c = 0.0$, which is a significant region in the hydroforming process under internal pressure and axial feeding. The lower value of plastic instability compared with that due to the other two criteria leads to an overestimate of the limit strains, as shown in Fig. 5, under the same loading condition. In a similar manner, in the range $\alpha < 0$, where compressive axial stresses are imposed due to axial feeding, it is expected that the limit strains based on the diffuse necking for a sheet will be underestimated compared with the others.

Figure 7 shows the analytically predicted bursting pressure, plotted as black square dots, experimentally obtained from bulge tests. The result for bursting pressure is similar to that for limit strain. The bursting pressure curve obtained from experimental

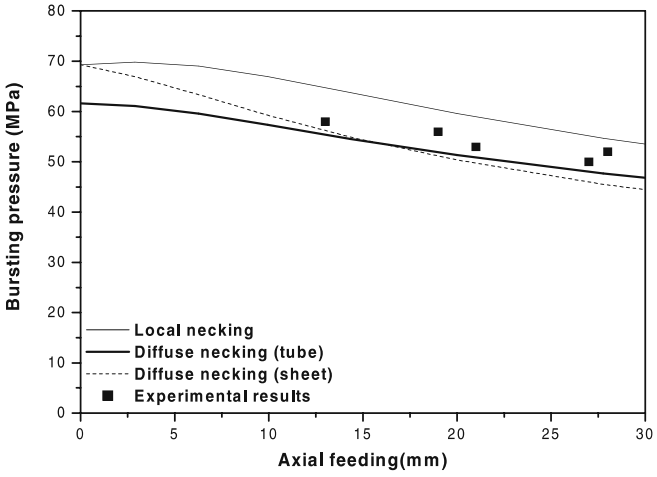

Fig. 7. Comparison of predicted and measured bursting pressures

results is below the curve based on the local necking criterion and above the curve based on diffuse necking criterion for a sheet. As a result of these findings, it can be concluded that a diffuse necking criterion for tube is more applicable for the prediction of the tubular hydroforming limit.

5 Influence of material properties on formability

From Eqs. 17 and 21, the influences of material properties on the plastic instability and bursting pressure are investigated. Figure 8 shows that the plastic instability expressed as $1/Z$ with respect to plastic anisotropy, R, strain-hardening exponent, n, and strength coefficient, K. To show the influence of the material properties on the plastic instability, $1/Z$ is plotted with respect to the following different variables: the stress ratio in Fig. 8a, the critical axial strain in Fig. 8b, and the critical axial stress in Fig. 8c. Although these properties have different physical meaning, the ranges of these variables on the horizontal axis plotted over Fig. 8a–c are compatible with each other. As shown in Fig. 8a, the plastic instability value $1/Z$decreases with an increase in R in both the tensile-compression and the biaxial stress zones. Figure 8b shows that $1/Z$ increases with an increase in n, and Fig. 8c shows that the plastic instability value $1/Z$ decrease with increasing K in the range of $\sigma_2 = 0$ MPa to $\sigma_2 = 700$ MPa while the opposite trend holds in the other region, which does not have a significant meaning in tube hydroforming with compressive axial feeding. These results mean that a large n makes it easy for plastic instability to occur; meanwhile, a large R and K can delay the onset of plastic instability.

In order to get an optimal loading path, under which there is no bursting failure during any hydroforming stage, the critical internal hydraulic pressures according to axial feeding for different material properties are calculated from Eq. 21 and depicted in Fig. 9. Any loading combination of internal pressure and axial feeding below the curve indicates no bursting failure expected. Figure 9a shows that the bursting pressure increases with increasing anisotropy parameter R, Fig. 9b shows that bursting pressure

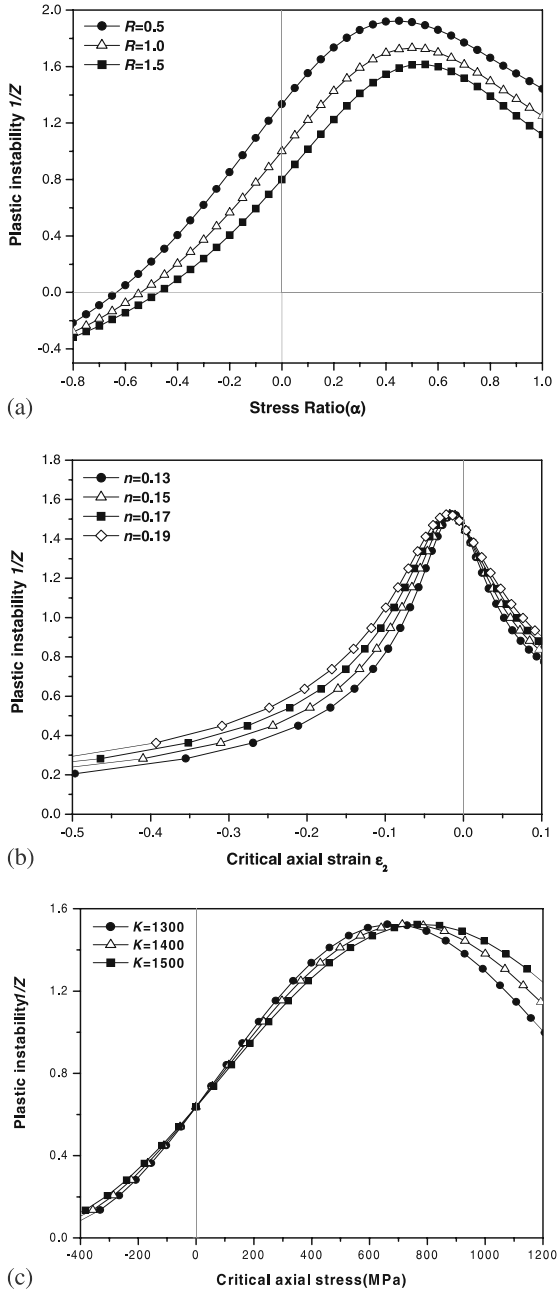

Fig. 8a–c. Effects of material properties on plastic instability. **a** Influence of anisotropy parameter, R. **b** Influence of strain hardening exponent, n. **c** Influence of strength coefficient, K

increases with decreasing n, and Fig. 9c shows that the forming window, which refers to the safe region under the bursting failure curve, increases with increasing K. These results shown in Fig. 9 are in good agreement with the influence of material properties on plastic instability shown in Fig. 8. It is noted that (i) the materials with large strain hardening coefficient, n, have a large limit strain; however, the corresponding stress value at that limit strain is smaller than that at the limit strain for materials with a

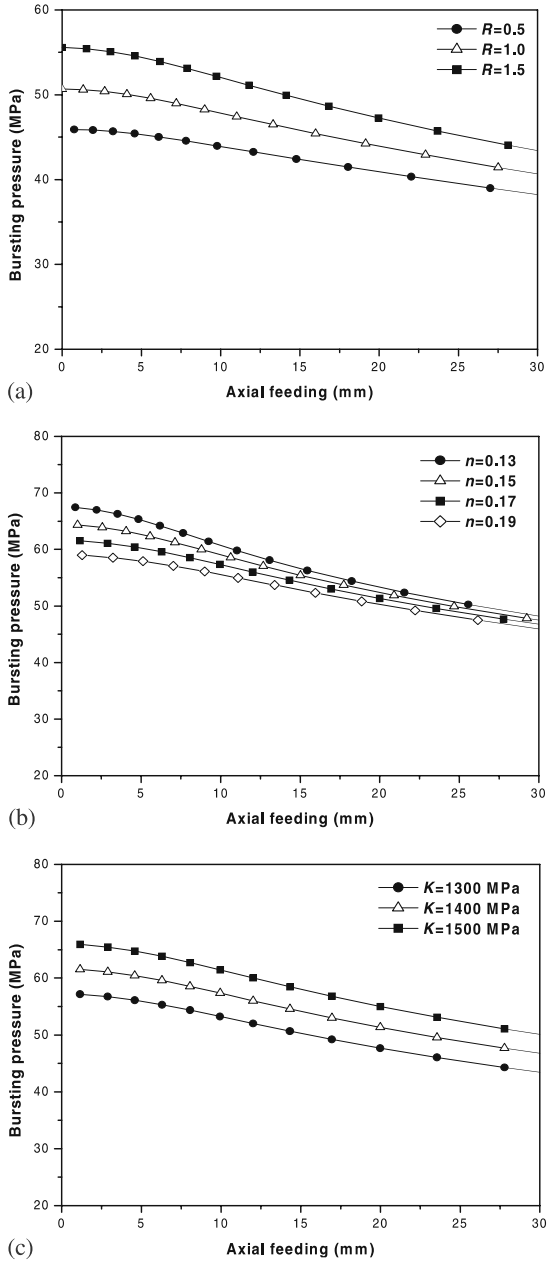

Fig. 9a–c. Effects of material properties on bursting pressure. **a** Influence of anisotropy parameter, R. **b** Influence of strain hardening exponent, n. **c** Influence of strength coefficient, K

lower n. It is easily demonstrated from the effective stress-strain curve obeying the work-hardening law, $\bar{\sigma} = K\bar{\varepsilon}^n$, that the effective stress decreases with increasing n in the region of strain less than 1.0. By reason of this effective stress-strain curve characteristic, bursting pressure calculated from Eq. 18 is decreased with increasing n by implying that formability of the material is increased. We also note that (ii) the effect of strength coefficient K on bursting pressure also can be explained by a simple stress-strain curve characteristic in the same manner. Finally, (iii) the influence of the plastic anisotropy parameter on bursting pressure observed from Fig. 9a can be explained by the fact that a large R-value makes it easy to deform in the hoop and axial directions compared with the thickness direction.

6 Conclusions

In this paper, three classical plastic instability criteria have been reviewed, and the potential for application of the predictions of the forming limit for tube hydroforming were investigated in view of bursting failures. In addition, the influences of material properties on plastic instability and bursting pressure are investigated.

Based upon both the analytical prediction and the experimental results, the following conclusions can be drawn:

- the prediction of the forming limit and bursting pressure reveals that the diffuse necking criterion for a tube is more applicable than the other plastic instability criteria investigated in this study.
- the plastic instability is reduced with decreasing strain hardening exponent, n, while it increases with decreasing plastic anisotropy parameter, R, and strength coefficient, K.
- the analytically predicted bursting pressure is reduced with increasing n-value while it increases with increasing K R.

Finally, comparison with the experimental results has shown that the limit strains and bursting pressures are successfully predicted using the proposed criteria. Therefore, it is expected that the analytical method developed here can be used as an effective tool for evaluating the formability in a wide range of practical tube hydroforming processes.

Acknowledgement This work has been completed with the support of 2003 Pusan National University Research Grant, for which the first author is grateful. The last author would like to acknowledge the support of the Brain Busan 21 Project.

References

1. Kang BS, Son BM, Kim J (2004) A comparative study of stamping and hydroforming processes for an automobile fuel tank using FEM. Int J Mach Tools Manuf 44:87–94
2. Yamada Y, Aoki I (1966) On the tensile plastic instability in axisymmetric deformation of sheet metals. J JSTP 67:393–406
3. Xing HL, Makinouchi A (2001) Numerical analysis and design for tubular hydroforming. Int J Mech Sci 43:1009–1026
4. Tirosh J, Neuberger A, Shirizly A (1996) On tube expansion by internal fluid pressure with additional compressive stress. Int J Mech Sci 38:839–851
5. Xia ZC (2001) Failure analysis of tubular hydroforming. J Eng Mater Technol 123:423–429
6. G. Nefussi, Combescure A (2002) A coupled buckling and plastic instability for tube hydroforming. Intl J Mech Sci 44:899–914
7. Kim J, Kim YM, Kang BS, Hwang SM (2004) Finite element analysis for bursting failure prediction in bulge forming of a seamed tube. Finite Elem Anal Des 40:953–966
8. Hill R (1983) The mathematical theory of plasticity. Oxford University Press, Oxford
9. Swift HW (1952) Plastic instability under plane stress. J Mech Phys Solids 1:1–18